journal

J. Am. Ceram. Soc., **81** [5] 1310–16 (1998)

Phase Relationships and Physical Properties of Homologous Compounds in the Zinc Oxide–Indium Oxide System

Toshihiro Moriga,*,† Doreen D. Edwards,* and Thomas O. Mason*

Department of Materials Science and Engineering and Materials Research Center, Northwestern University, Evanston, Illinois 60208-3108

George B. Palmer and Kenneth R. Poeppelmeier*

Department of Chemistry and Materials Research Center, Northwestern University, Evanston, Illinois 60208-3113

Jon L. Schindler‡ and Carl R. Kannewurf

Department of Electrical and Computer Engineering, Northwestern University, Evanston, Illinois 60208-3118

Ichiro Nakabayashi

Department of Chemical Science and Technology, Faculty of Engineering, Tokushima University, Tokushima 770, Japan

Equilibrium phase relationships in the $ZnO–In_2O_3$ system were determined between 1100° and 1400°C using solid-state reaction techniques and X-ray diffractometry. In addition to ZnO and In_2O_3, nine homologous compounds, $Zn_kIn_2O_{k+3}$ (where k = 3, 4, 5, 6, 7, 9, 11, 13, and 15), were observed. Electrical conductivity and diffuse reflectance of the k = 3, 4, 5, 7 and 11 members were measured before and after annealing at 400°C for 1 h under forming gas (4% H_2–96% N_2). Room-temperature conductivity increased as k decreased, because of increased carrier concentration as well as increased mobility. In general, transparency in the wavelength range of 450–900 nm increased as k increased. Reduction in forming gas resulted in increased conductivity and reduced transparency for all compounds measured. The highest room-temperature conductivity measured, 270 S/cm, was that of reduced $Zn_3In_2O_6$.

I. Introduction

TRANSPARENT conducting oxides, or TCOs, are widely used as transparent electrodes for flat panel displays and solar cells. Commercial, thin-film tin-doped indium oxide, or ITO, exhibits a conductivity of 1000–5000 S/cm and an optical transparency of 85%–90%.[1] Nevertheless, alternative materials with higher conductivity, better transparency at blue-green wavelengths, and lower cost are desired. There have been several recent reports of thin-film TCOs in the $ZnO–In_2O_3$ system, demonstrating that high transparency and high conductivity can be achieved for a wide range of film compositions. Wang *et al.*[2] reported conductivities as high as 1100 S/cm for sputtered ZnO films containing <5 at.% indium.[2] Minami and coworkers[3,4] reported conductivities as high as 2900 S/cm for $Zn_2In_2O_5$ films sputtered from polycrystalline targets containing 10–60 at.% zinc. In studies of pulse-laser-deposited tin-doped films, Phillips *et al.*[5] reported conductivities as high as 2500 S/cm for films with a [Zn]:([In] + [Sn]) ratio of 0.5–0.6.

Although nonequilibrium conditions often exist during thin-film deposition, knowledge of equilibrium phase relationships and bulk, physical properties of stable phases can be helpful in interpreting and directing thin-film work. Although it is well documented that ZnO and In_2O_3 react to form several stable compounds, a complete phase diagram of the $ZnO–In_2O_3$ system has not been reported. Furthermore, there are few reports regarding the electrical and optical properties of $ZnO–In_2O_3$ phases. In this study, we present the $ZnO–In_2O_3$ phase diagram for 1100°–1400°C. We also characterize the electrical and optical properties of five $ZnO–In_2O_3$ phases to investigate the compositional dependency of properties important for TCO applications.

ZnO and In_2O_3 react at high temperatures (>1000°C) to form a series of homologous compounds, $Zn_kIn_2O_{k+3}$, where k is an integer. Kasper[6] demonstrated the formation of k = 2–5 and 7 members at 1100°–1550°C but could not obtain the spinel (k = 1), even at temperatures as high as 1750°C. Nakamura *et al.*[7] reported that $Zn_kIn_2O_{k+3}$ (k = 3, 4, 5, 6, 7, 8, 9, 11, 13, and 15) are stable at 1350°C and that $Zn_kIn_2O_{k+3}$ (k = 20) forms at 1550°C. They also speculated that an infinite number of phases could exist between the k = 20 member and ZnO. Kimizuka *et al.*[8] reported the formation of k = 3–5, 7, 9, and 11 members at 1150°–1550°C. The temperature range of stability of most of the $Zn_kIn_2O_{k+3}$ members has not been reported.

ZnO crystallizes in the hexagonal wurtzite structure with a = 3.2498 Å and c = 5.2066 Å (JCPDS§ Card No. 36-1451). In_2O_3 crystallizes in the C-M_2O_3 (bixbyite) structure with a = 10.117 Å (JCPDS Card No. 6-416). The homologous $Zn_kIn_2O_{k+3}$ compounds crystallize in R-3m, for odd k values with z = 3, and in $P6_3/mmc$, for even k values with z = 2

N. J. Dudney—contributing editor

Manuscript No. 191148. Received March 11, 1997; approved July 15, 1997.

Supported by the MRSEC Program of the National Science Foundation (under Contract No. DMR-9632472) at the Materials Research Center of Northwestern University. This work made use of the Central Facilities, which were also supported by the same MRSEC program. Author TM, on sabbatical at Northwestern University during the time of the study, was supported by a Research Fellowship from the Ministry of Education of Japan. Author GBP was supported by a National Defense Science and Engineering Graduate Fellowship from the U.S. Office of Naval Research.

*Member, American Ceramic Society.

†Permanent address: Department of Chemical Society and Technology, Faculty of Engineering, Tokushima University, Tokushima 770, Japan.

‡Permanent address: CMRC–Display Technologies Group, Motorola, Schaumburg, IL 60196.

§Joint Committee on Powder Diffraction Standards, Swarthmore, PA (now International Centre for Diffraction Data (ICDD), Newtowne Square, PA).

(where z is the number of formula units per unit cell). The structures are characterized by a short ***a***-axis (3.2–3.4 Å) and a long ***c***-axis (e.g., 42.5 Å for $k = 3$ and 33.5 Å for $k = 4$). Based on high-resolution electron microscopy results, Cannard and Tilley[9] proposed that the structures consist of k ZnO layers separated by two $InO_{1.5}$ layers, arranged such that $[001]_{ZnO}$ and $[111]_{In_2O_3}$ are parallel to [001] of the $Zn_kIn_2O_{k+3}$ structures. More recently, Nakamura *et al.*[7] and Kimizuka *et al.*[8] suggested that the compounds are isostructural with $LuFeO_3(ZnO)_k$. Although the two models are not identical, both feature wurtzite-type layers perpendicular to the ***c***-axis of the $Zn_kIn_2O_{k+3}$ structures.

ZnO and In_2O_3 exhibit n-type semiconductivity. For ZnO and indium-doped ZnO powders, Wang *et al.*[10] reported conductivities ranging from 0.0001 to 30 S/cm. Ohta *et al.*[11] reported that $Zn_kIn_2O_{k+3}$ ($k = 5$, 7, and 9) are also n-type semiconductors, with conductivities on the order of 100–300 S/cm at 227°–727°C. Phillips *et al.*[5] reported a room-temperature conductivity of ~550 S/cm for bulk, reduced $Zn_3In_{1.975}Sn_{0.025}O_6$.

II. Experimental Procedure

A series of compositions were prepared from In_2O_3 and ZnO powders (>99.9% purity, on a cation basis, Aldrich Chemical Co., Milwaukee, WI). Weighed amounts of the dried starting powders were ground together with a mortar and pestle, to provide a series of samples with integral Zn:In ratios ranging from 1 to 15. The mixed powder was calcined at 1000°C overnight in air and then reground. Pellets pressed from this powder were heated in covered high-density alumina crucibles. The grinding and heating steps were repeated as necessary to attain equilibrium, as determined by X-ray diffractometry (XRD). The total heating times were 7–10 days at ≤1100°C, 7 days at 1101°–1249°C, 5 days at 1250°C, 4 days at 1251°–1300°C, and 3–4 days at ≥1300°C. Each pellet was sandwiched between sacrificial pellets or surrounded by powder of the same composition, to minimize contamination from the alumina crucible and to inhibit vaporization of ZnO during firing. Weight loss during firing was typically <0.8%. After heating at the desired temperature, the samples were removed from the furnace at temperature and cooled in ambient air, resulting in room-temperature pellets in ~20 min. The phase composition was determined by powder XRD (Scintag, Santa Clara, CA) using Cu$K\alpha$ radiation (40 kV, 20 mA). Commercial software (Scintag) was used to remove the background and Cu$K\alpha_2$ contributions from the diffraction patterns.

Electrical conductivity and diffuse reflectance of sintered pellets were measured before and after reduction in forming gas (4% H_2–96% N_2) at 400°C for 1 h. The $Zn_kIn_2O_{k+3}$ pellets used for these tests were reacted/sintered at 1400°C and had relative densities near 50% of theoretical. For comparison to the homologous compounds, ZnO and In_2O_3 pellets were also examined. The In_2O_3, sintered at 1400°C, was similar to the homologous compounds, in terms of density and color. ZnO sintered at 1400°C was black, indicating severe reduction, and had a density that was >95% of the theoretical density. Sinter-

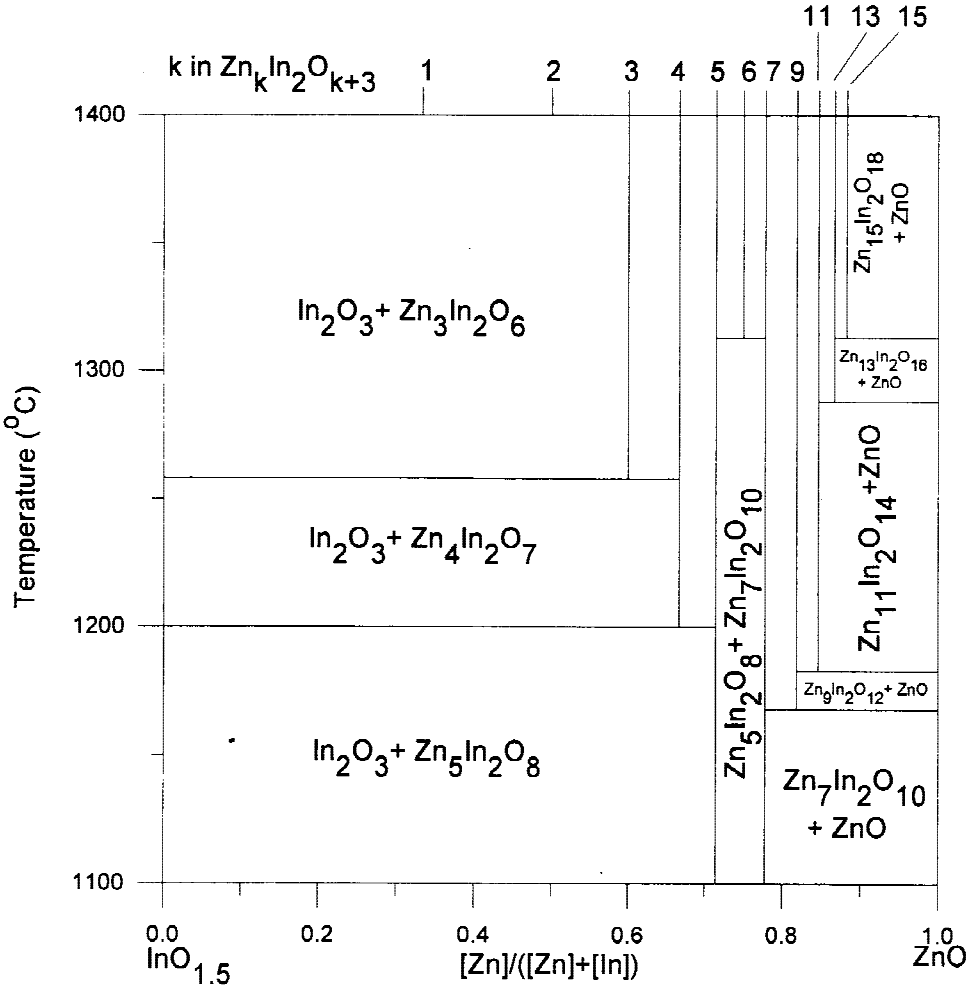

Fig. 1. Phase diagram for the In_2O_3–ZnO system over the temperature range of 1100°–1400°C.

Table I. Phase Analysis of Prepared Compositions

Indium concentration, [In]	Reaction temperature (°C)†													
	1100	1150	1160	1175	1190	1200	1215	1250	1265	1275	1300	1325	1350	1400
0.02	0 + 5					0 + 4					0 + 3			0 + 3
0.20	0 + 5	0 + 5			0 + 5	0 + 4	0 + 4	0 + 4	0 + 3		0 + 3		0 + 3	0 + 3
0.33	0 + 5	0 + 5			0 + 5	0 + 4	0 + 4	0 + 4	0 + 3		0 + 3		0 + 3	0 + 3
0.50	0 + 5	0 + 5			0 + 5	0 + 4	0 + 4	0 + 4	0 + 3		0 + 3		0 + 3	0 + 3
0.60	0 + 5	0 + 5			0 + 5	0 + 4	0 + 4	0 + 4	3		3		3	3
0.63	0 + 5					0 + 4	0 + 4	0 + 4	3 + 4		3 + 4		3 + 4	3 + 4
0.67	0 + 5	0 + 5			0 + 5	4	4	4	4		4		4	4
0.69						4 + 5	4 + 5	4 + 5	4 + 5		4 + 5		4 + 5	4 + 5
0.71	5	5		5	5	5	5	5	5		5	5	5	5
0.73												5 + 6		5 + 6
0.75	5 + 7	5 + 7		5 + 7		5 + 7		5 + 7			5 + 7	6	6	6
0.76												6 + 7		6 + 7
0.78	7	7	7	7	7	7		7			7	7	7	7
0.80				7 + 9	7 + 9	7 + 9		7 + 9			7 + 9	7 + 9	7 + 9	7 + 9
0.82	7 + ∞	7 + ∞		9	9	9		9		9	9	9	9	9
0.83			7 + ∞		9 + 11	9 + 11		9 + 11		9 + 11	9 + 11		9 + 11	9 + 11
0.85					11	11		11		11	11	11	11	11
0.86										11 + ∞	11 + 13			11 + 13
0.87					11 + ∞	11 + ∞		11 + ∞			13	13	13	13
0.875												13 + 15		13 + 15
0.88						11 + ∞		11 + ∞			13 + ∞	15	15	15
0.91												15 + ∞	15 + ∞	15 + ∞
0.95	7 + ∞	7 + ∞	7 + ∞	11 + ∞	11 + ∞	11 + ∞		11 + ∞			13 + ∞	15 + ∞	15 + ∞	15 + ∞

†Integers greater than zero indicate k in $Zn_kIn_2O_{k+3}$, ''0'' indicates In_2O_3, and ''∞'' indicates ZnO.

ing at 800°C for 15 min provided a ZnO pellet with a relative density similar to that of the homologous compounds.

The room-temperature electrical conductivity was measured with a linear four-point probe using a current source and voltmeter (Models 225 and 197, Keithley Instruments, Cleveland, OH). Excitation currents ranged from 100 nA to 10 mA. The conductivity was calculated as

$$\sigma = \frac{1}{\rho} = \frac{1}{\frac{V}{I} wC\left(\frac{d}{s}\right)F\left(\frac{w}{s}\right)}$$

where σ is the conductivity, ρ the resistivity, V the voltage, I the current, w the pellet width, d the pellet diameter, and s the electrode spacing; $C(d/s)$ and $F(w/s)$ are correction factors that account for sample geometry and finite thickness, respectively.[12] The room-temperature Hall effect and conductivity measurements of the reduced $Zn_kIn_2O_{k+3}$ compounds were made on rectangular, bar-shaped samples cut from the reduced pellets. Electrical contacts to the bars were prepared with small indium dots. Gold sample leads (60 or 25 μm in diameter) were bonded to the indium contacts with silver paste. The Hall measurements used magnetic flux densities of ~8000 G (0.8 T) and measurement currents of 0.1–2.0 mA, depending on the sample response. All voltages were measured using a nanovoltmeter (Model 182, Keithley). The conductivity values measured for the bar-shaped samples agreed within 20% of those determined by the linear four-point probe. To account for the variation in the densities among the measured samples, carrier concentration and conductivity values were divided by the relative density of the corresponding sample. Therefore, the conductivities reported in this paper are roughly 2 times larger than the actual measured values.

Diffuse reflectance was measured from 200 to 900 nm using a double-beam spectrophotometer with integrating sphere (Model Cary 1E with Cary 1/3 attachment, Varian, Palo Alto, CA). Baseline spectra were collected with pressed polytetrafluoroethylene (PTFE) powder compacts (Varian Part No. 04-101439-00) placed in the sample and reference beams. Sample measurements on as-fired and as-annealed pellets, with no further surface preparation, were made in reference to the PTFE standards.

III. Results and Discussion

Figure 1 shows the phase diagram of the ZnO–In_2O_3 system, from 1100° to 1400°C. The phase diagram is similar to the Ga_2O_3–TiO_2 system, which also contains several homologous compounds.[13] In accordance with the equilibrium phase rule, the diffraction patterns used to construct this diagram showed only one or two phases, as summarized in Table I. In addition to ZnO and In_2O_3, nine homologous compounds, summarized in Table II, were detected. The lower limit of temperature stability (T_{low}) (Table II) is given as the midpoint between the lowest firing temperatures at which the corresponding compound was observed and the highest firing temperature at which the corresponding compound did not form. The large uncertainty shown for T_{low} in Table II results from the temperature intervals used in this study, typically 15°–25°C. To confirm that the small number of compounds observed at the lowest temperatures was not due to kinetic limitations of the In_2O_3–ZnO reaction, $Zn_3In_2O_6$ samples were annealed at 1100° and 1250°C, for 3 weeks and 1 week, respectively, resulting in partial decomposition, which is consistent with the phase relationships shown in Fig. 1.

In Fig. 1, line compounds, rather than regions of solid solution, are shown, because the lattice parameters measured for the homologous compounds in the biphasic mixtures were

Table II. Lower Limit of Stability (T_{low}) and Lattice Constants of $Zn_kIn_2O_{k+3}$ Compounds

k value in $Zn_kIn_2O_{k+3}$	T_{low} (°C)†	Lattice parameter (Å)†		Normalized lattice parameter, c (Å)/z
		a	c	
3	1258 (8)	3.353 (1)	42.50 (1)	14.17
4	1200 (10)	3.338 (1)	33.52 (1)	16.76
5	≤1100	3.326 (1)	58.10 (1)	19.37
6	1313 (13)	3.316 (1)	43.95 (1)	21.98
7	≤1100	3.311 (1)	73.68 (1)	24.56
9	1168 (8)	3.300 (1)	89.24 (1)	29.75
11	1183 (8)	3.291 (1)	104.95 (1)	34.98
13	1288 (13)	3.284 (1)	120.36 (1)	40.12
15	1313 (13)	3.278 (1)	135.98 (1)	45.33

†Numbers given in parentheses are estimated uncertainties.

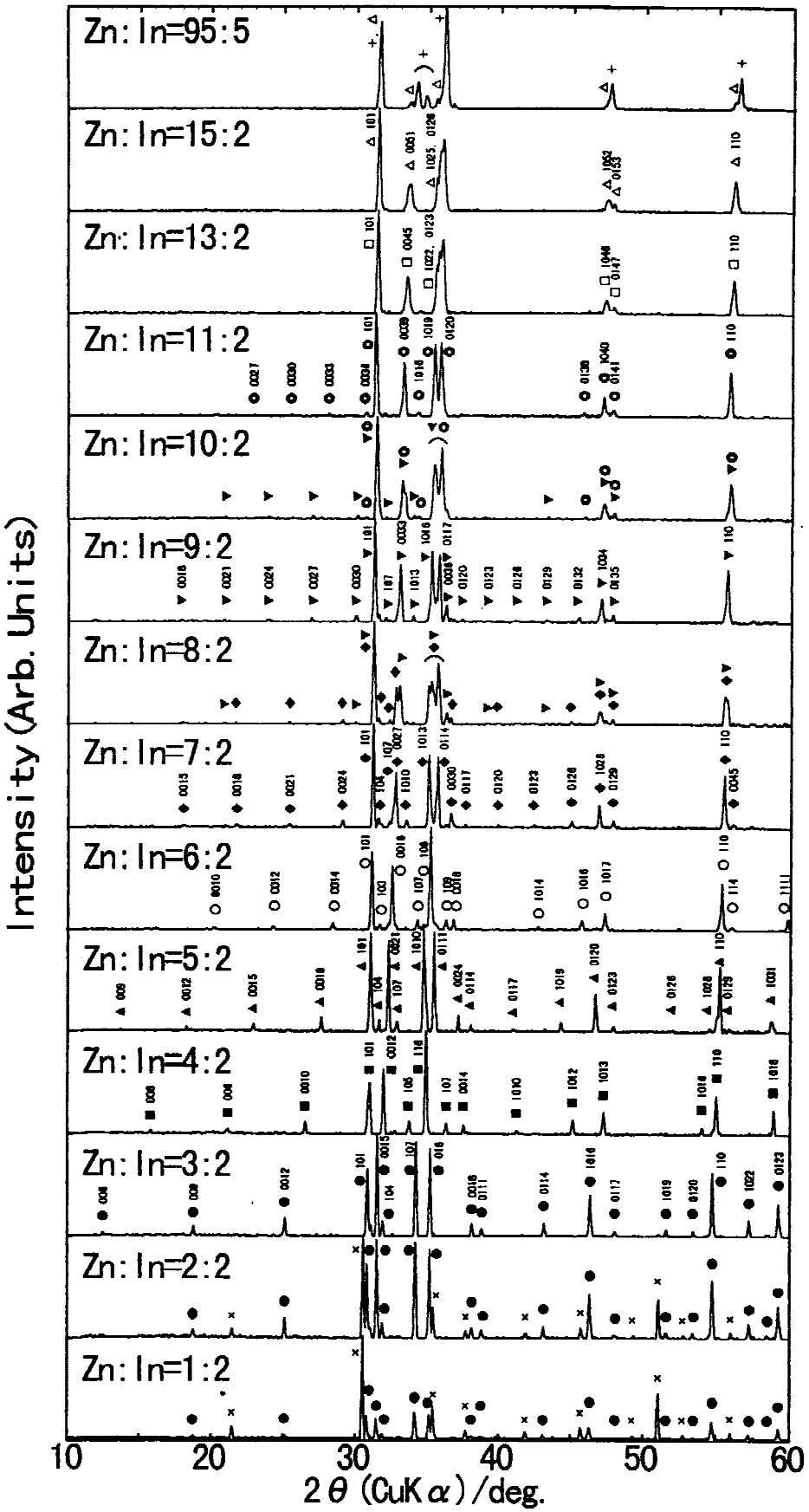

Fig. 2. X-ray diffractograms for ZnO–In_2O_3 compositions reacted at 1400°C. Peaks are indexed as (*hkl*) or (*hkll*) ((×) In_2O_3, (●) $Zn_3In_2O_6$, (■) $Zn_4In_2O_7$, (◀) $Zn_5In_2O_8$, (○) $Zn_6In_2O_{10}$, (◆) $Zn_7In_2O_{11}$, (▶) $Zn_9In_2O_{12}$, (⏺) $Zn_{11}In_2O_{14}$, (□) $Zn_{13}In_2O_{16}$, (◁) $Zn_{15}In_2O_{18}$, and (+) ZnO).

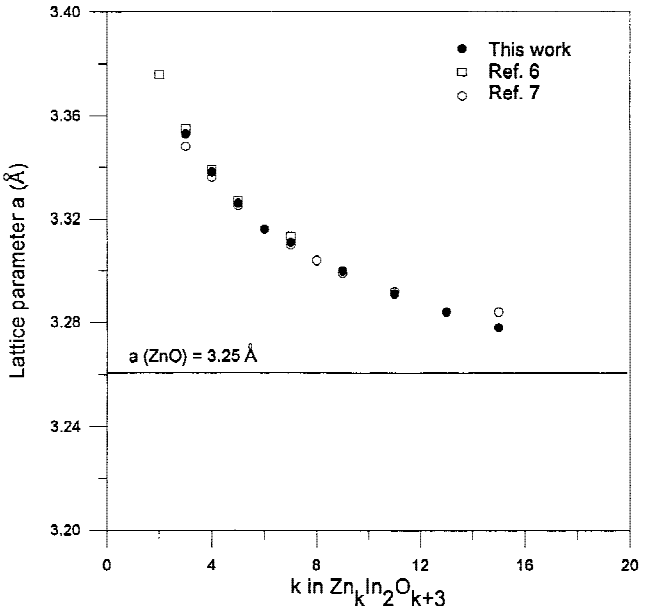

Fig. 3. Lattice constant *a*, as a function of *k* in $Zn_kIn_2O_{k+3}$.

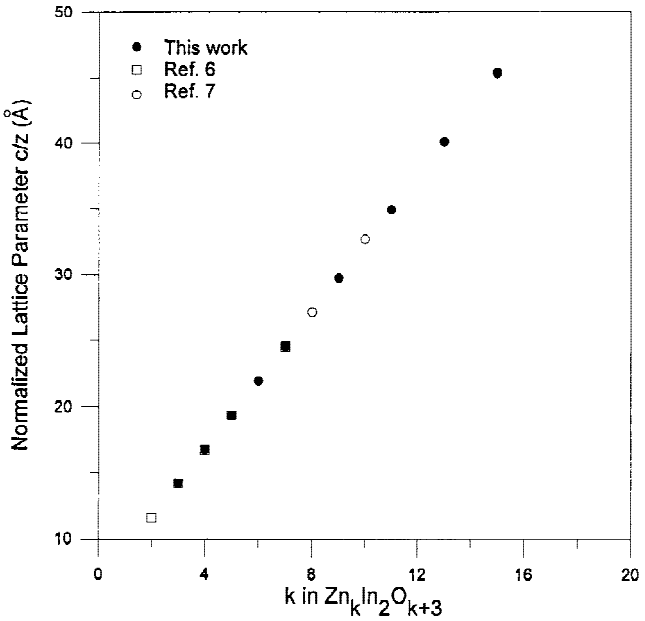

Fig. 4. Normalized lattice constant (*c*/*z*), as function of *k* in $Zn_kIn_2O_{k+3}$.

identical, within experimental uncertainty, to those of the corresponding single-phase materials. Wang *et al.*[10] reported that up to 0.45 at.% indium is incorporated in ZnO processed at 1200°C. Considering the structural similarity between the homologous compounds and ZnO, we recognize that narrow regions of solid solution may exist.

The diagram shown in Fig. 1 is in disagreement with the conclusions drawn by Nakamura *et al.*,[7] who reported that $Zn_8In_2O_{11}$ and possibly $Zn_{10}In_2O_{13}$ are stable phases at 1350°C. Figure 2 shows the XRD patterns obtained for compositions heated at 1400°C. For higher-order members of the series, the peak overlap in the interval $32° \leq 2\theta \leq 40°$ makes it somewhat difficult to distinguish between successive members of the homologous series. Nevertheless, from the X-ray patterns, we are confident that the sample prepared with a Zn:In ratio of 8:2 consists of $Zn_7In_2O_{10}$ and $Zn_9In_2O_{12}$ and that the sample prepared with a Zn:In ratio of 10:2 consists of $Zn_9In_2O_{12}$ and $Zn_{11}In_2O_{14}$. Although the diffraction pattern of the sample prepared with a Zn:In ratio of 95:5 ($k = 38$) is consistent with a biphasic mixture of ZnO and $Zn_{15}In_2O_{18}$, the presence of higher-order members of the $Zn_kIn_2O_{k+3}$ series would be almost impossible to detect with the XRD technique used in this study. Therefore, additional homologous members with $k > 15$ may be stable at this temperature.

The lattice constants determined in this study, also summarized in Table II, agree well with values reported in the literature.[6–8] Figure 3 shows that the lattice parameter *a* decreases as *k* increases, from $a = 3.353$ Å for $k = 2$ to a value approaching that of wurtzite-type ZnO ($a = 3.250$ Å). This trend reflects the increasing influence of the ZnO layers in defining the ***a***-axis of the homologous compounds. To make meaningful comparisons among members of the homologous series, the lattice parameter *c* is divided by the number of formula units per unit cell (*z*). Figure 4 shows that the normalized lattice parameter, *c*/*z*, increases linearly as *k* increases, at a rate of 2.6 Å/*k*, which corresponds to one-half of the lattice constant *c* of ZnO, i.e., one Zn–O layer.

The color of the $Zn_kIn_2O_{k+3}$ compounds fired at 1400°C ranged from dark yellow-green to light canary yellow with increasing zinc content. The samples calcined at 1100°C were generally lighter than higher-temperature samples, with colors ranging from dark to light yellow with increasing zinc content. Figure 5 shows the diffuse reflectance spectra of $Zn_kIn_2O_{k+3}$ ($k = 3$, 4, 5, 7, and 11) prepared at 1400°C before and after reduction. Diffuse reflectance spectra of bulk samples are analogous to transmission spectra of thin samples.[14] All samples exhibit a transition from absorbing behavior at $\lambda < 400$ nm to transmitting (reflecting) behavior at $\lambda > 450$ nm. Based on the onset of diffuse reflection, the band gaps of $Zn_kIn_2O_{k+3}$ ($k = 3$, 4, 5, 7, and 11) are estimated to be 2.8–3.0 eV, which is in good agreement with a value of 2.9 eV reported for $Zn_2In_2O_5$.[3,4] Table III shows that the absorption edge decreases, or the band gap increases, as *k* increases. Reduction in forming gas results in an increase in the band gap. This phenomenon, known as the Burstein–Moss shift, has been observed in many TCO materials and results from increased carrier concentration.[15] For the as-fired samples, transparency at $\lambda > 450$ nm increases as *k* increases. For each of the compounds, transparency decreases upon reduction in forming gas.

Table III and Fig. 6 show that the electrical conductivity of the $Zn_kIn_2O_{k+3}$ compounds decreases as *k* increases. Hall effect measurements of the reduced $Zn_kIn_2O_{k+3}$ samples indicate that the decrease in conductivity results from decreased carrier concentration as well as decreased mobility. Reduction in forming gas (low oxygen partial pressure) results in increased conductivity for all the compounds, presumably because of the formation of oxygen vacancies, which serve as electron donors. The effect of reduction on the resulting conductivity increases as *k* increases for the $Zn_kIn_2O_{k+3}$ compounds. For example, the conductivity of $Zn_7In_2O_{10}$ increases by more than 2 orders of magnitude on reduction, whereas that of $Zn_3In_2O_6$ is only doubled.

Examination of the similarities and differences among the homologous compounds and parent oxides is the first step toward understanding the defect chemistry of the $Zn_kIn_2O_{k+3}$ materials. Based on the layered structural models proposed for the homologous compounds, we anticipated that the electrical properties would be intermediate between that of In_2O_3 and ZnO, approaching those of ZnO with increasing *k*; however, this was not strictly the case. The lowest-order member examined in this work, $Zn_3In_2O_6$ ($k = 3$), is similar to In_2O_3 ($k = 0$), in terms of color and conductivity before and after reduction in forming gas (see Fig. 6). In the oxidized state, the colors of the homologous compounds become lighter with increasing *k*, a trend that is consistent with the white color of well-oxidized ZnO ($k = \infty$). However, ZnO sintered at 1400°C (the same temperature used to process the homologous compounds) was black and had a conductivity of ~10 S/cm, indicating considerable reduction. From this observation, we conclude that, al-

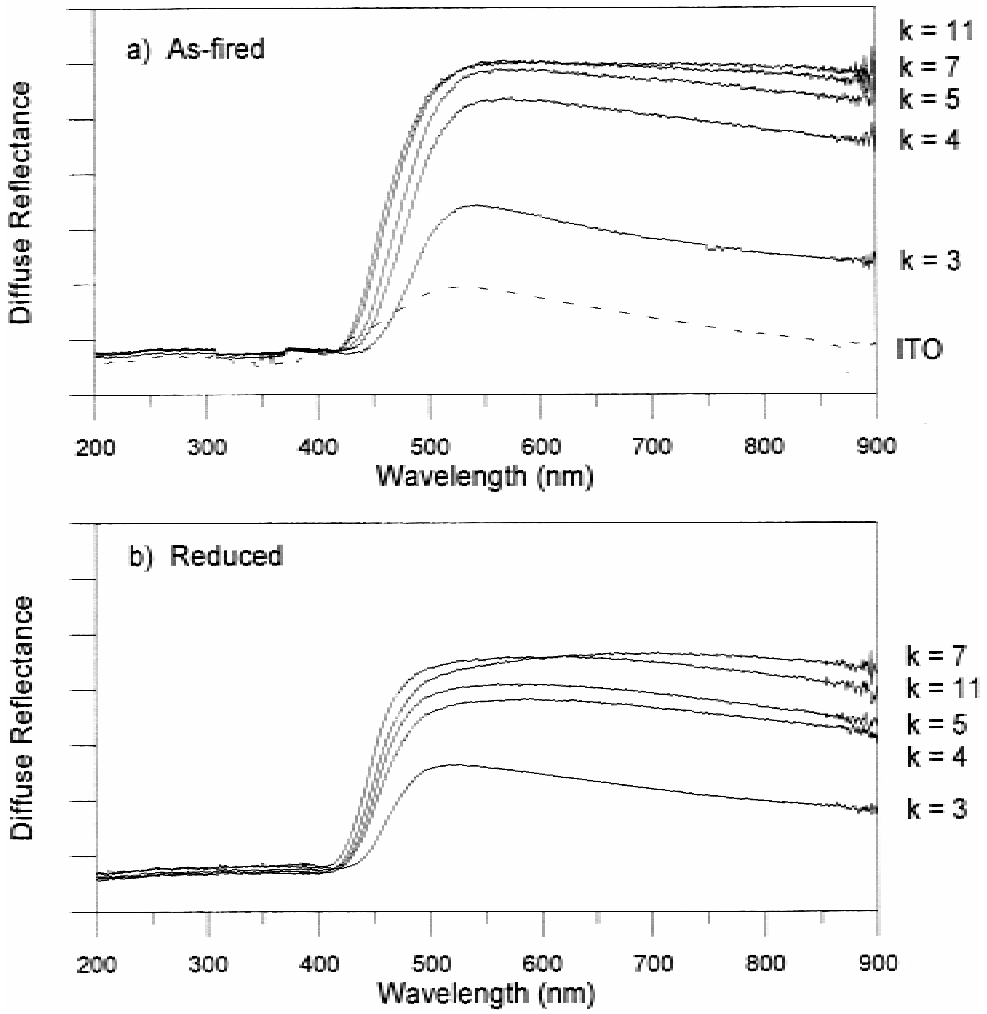

Fig. 5. Diffuse-reflectance spectra for $Zn_kIn_2O_{k+3}$ (k = 3, 4, 5, 7, and 11) compounds and ITO (3% tin) ((a) after firing at 1400°C and (b) after reduction in forming gas at 400°C).

Table III. Electrical and Optical Properties of Select $Zn_kIn_2O_{k+3}$ Compounds

k value in $Zn_kIn_2O_{k+3}$	Absorption-edge λ (nm)		Conductivity, σ (S/cm)		Mobility, μ (reduced) ($cm^2 \cdot (V \cdot s)^{-1}$)	n (reduced) ($\times 10^{19}$ cm^{-3})
	As-fired	Reduced	As-fired	Reduced		
3	442	437	120	270	25.1	6.63
4	435	420	6.0	100	13.7	4.65
5	432	418	0.9	53	12.2	2.75
7	423	415	0.1	19	11.3	1.83
11	420	410		6.7	4.5	0.93

though the higher-order $Zn_kIn_2O_{k+3}$ are believed to contain a considerable volume fraction of ZnO-like layers, their susceptibility to reduction at high temperature and ambient atmosphere is lower than that of ZnO. A porous ZnO pellet, sintered at 800°C, was white and insulating, consistent with trends observed for the higher-k members of the homologous series (see Fig. 6). However, a significant increase in the conductivity of ZnO was not observed after reduction, as was the case for $Zn_{11}In_2O_{14}$, the highest-order member of the series studied. Continued efforts are underway to understand the defect chemistry of the $Zn_kIn_2O_{k+3}$ compounds, in terms of the layered structure model and the parent compounds.

The results of this work provide some insight for developing TCOs based on the $Zn_kIn_2O_{k+3}$ compounds. Although the optical properties desired for TCO applications improve with increasing k, the electrical properties desired for TCO applications improve with decreasing k. Nevertheless, as shown in Fig. 5, all the homologous compounds examined are superior to bulk ITO (3% tin, processed at 1250°C) insofar as diffuse reflectance (transmittance) is concerned. Of the compounds examined, $Zn_3In_2O_6$ has the highest conductivity, which is an order of magnitude lower than that desired for TCO applications. Hall measurements indicate that this results from a low carrier concentration rather than a low mobility, e.g., the values measured for $Zn_3In_2O_6$ (6.7×10^{19} cm^{-3} and 25.1 $cm^2 \cdot (V \cdot s)^{-1}$, respectively) versus the values reported for commercial TCO thin films (6.6×10^{20}–1.2×10^{21} cm^3 and 10.2–28.3 $cm^2 \cdot (V \cdot s)^{-1}$, respectively).[1] Excluding In_2O_3 from consideration, the increase in conductivity with decreased k suggests that lower-order members of the series, $Zn_kIn_2O_{k+3}$ (k = 1 and 2), may have higher conductivities than that of $Zn_3In_2O_6$. Although $Zn_2In_2O_5$ has been reported to form at >1550°C[6] and has been observed in thin-film studies,[3,4] the formation of $ZnIn_2O_4$ has not been reported. Strategies to increase the con-

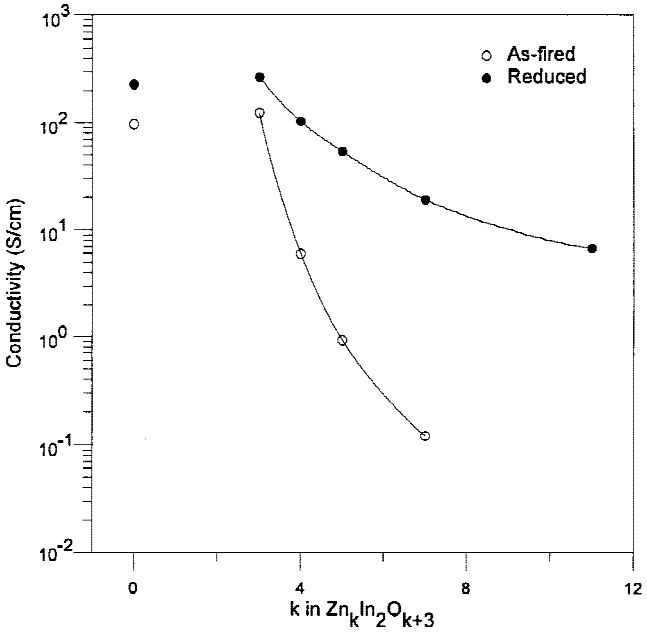

Fig. 6. Room-temperature electrical conductivity before and after reduction in forming gas (4% H_2–96% N_2).

ductivity of the $Zn_kIn_2O_{k+3}$ compounds (stabilization of lower-k members, doping with aliovalent cations, and optimized annealing conditions) are currently being explored.

IV. Conclusions

The subsolidus phase diagram for the ZnO–In_2O_3 system over the temperature range of 1100°–1400°C was presented. In addition to In_2O_3 and ZnO, nine homologous compounds were observed—$Zn_kIn_2O_{k+3}$, where k = 3, 4, 5, 6, 7, 9, 11, 13, and 15. At 1100°C, $Zn_5In_2O_8$ and $Zn_7In_2O_{10}$ were the only stable compounds other than the component oxides; however, the number of stable compounds increased as the temperature increased. Overall, the temperature ranges of stability determined in this study were in fair agreement with the previously reported literature.[6–8] The major exception was that the k = 8 or k = 10 members of the series were not observed over the temperature range studied.

Trends in electrical conductivity and optical transparency, as functions of k in $Zn_kIn_2O_{k+3}$, were identified. The electrical conductivity increased as k decreased, as a result of increased carrier concentration as well as increased carrier mobility. For all the compounds examined, reduction in forming gas resulted in increased conductivity; however, the magnitude of the effect increased as k increased. The optical band gap and transparency in the visible region increased as k increased. Reduction in forming gas resulted in decreased transparency and a widening of the band gap (the Burstein–Moss shift).

References

[1]N. R. Lyman, ''Transparent Electronic Conductors''; pp. 201–31 in *Proceedings of the Symposium on Electrochromic Materials*, Electrochemical Society Proceedings, Vols. 90–92. Electrochemical Society, Princeton, NJ, 1990.

[2]R. Wang, L. H. L. King, and A. W. Sleight, ''Highly Conducting Transparent Thin Films Based on Zinc Oxide,'' *J. Mater. Res.*, **11** [7] 1659–64 (1996).

[3]T. Minami, T. Kakumu, and S. Tanaka, ''Preparation of Transparent and Conductive In_2O_3–ZnO Films by Radio Frequency Magnetron Sputtering,' *J. Vac. Sci. Technol.*, A, **14** [3] 1704–708 (1996).

[4]T. Minami, H. Sonohara, T. Kakumu, and S. Tanaka, ''Highly Transparent and Conductive $Zn_2In_2O_5$ Thin Films Prepared by RF Magnetron Sputtering,'' *Jpn. J. Appl. Phys., Part 2*, **34** [8A] L971–L974 (1995).

[5]J. M. Phillips, R. J. Cava, G. A. Thomas, S. A. Carter, J. Kwo, T. Siegrist, J. J. Krajewski, J. H. Marshall, W. F. Peck Jr., and D. H. Rapkine, ''Zinc-Indium-Oxide: A High Conductivity Transparent Conducting Oxide,'' *Appl. Phys. Lett.*, **67** [15] 2246–48 (1994).

[6]V. H. Kasper, ''Neuartige Phasen mit Wurtzitahnlichen Strukturn im System ZnO–In_2O_3,'' *Z. Anorg. Allg. Chem.*, **349** [3–4] 113–224 (1967).

[7]N. Nakamura, M. Kimizuka, and T. Mohri, ''The Phase Relation in the In_2O_3–Fe_2ZnO_4–ZnO System at 1350°C,'' *J. Solid State Chem.*, **86**, 16–40 (1990).

[8]N. Kimizuka, M. Isobe, and M. Nakamura, ''Synthesis and Single-Crystal Data of Homologous Compounds, $In_2O_3(ZnO)_m$ (m = 3, 4, and 5), $InGaO_3(ZnO)_3$, and $Ga_2O_3(ZnO)_m$ (m = 7, 8, 9, and 16) in the In_2O_3–$ZnGa_2O_4$–ZnO System,'' *J. Solid State Chem.*, **116**, 170–78 (1994).

[9]P. J. Cannard and R. J. D. Tilley, ''New Intergrowth Phases in the ZnO–In_2O_3 System,'' *J. Solid State Chem.*, **73**, 418–26 (1988).

[10]R. Wang, A. W. Sleight, R. Platzer, and J. A. Gardner, ''Nonstoichiometric Zinc Oxide and Indium-Doped Zinc Oxide: Electrical Conductivity and ^{111}In-TDPAC Studies,'' *J. Solid State Chem.*, **122**, 166–75 (1996).

[11]H. Ohta, W.-S. Seo, and K. Koumoto, ''Thermoelectric Properties of Homologous Compounds in the ZnO–In_2O_3 System,'' *J. Am. Ceram. Soc.*, **79** [8] 2193–96 (1996).

[12]F. M. Smits, ''Measurement of Sheet Resistivities with the Four-Point Probe,'' *Bell Syst. Tech. J.*, **37** [3] 711–18 (1958).

[13]L. A. Bursill and G. G. Stone, ''Tunnel and Intergrowth Structures in the Gallia-rich Gallium Titanate System,'' *J. Solid State Chem.*, **38**, 149–57 (1981).

[14]H. G. Hecht, ''The Present Status of Diffuse Reflectance Theory''; pp. 1–26 in *Modern Aspects of Reflectance Spectroscopy.* Edited by W. W. Wendlandt. Plenum Press, New York, 1968.

[15]I. Hamberg and C. G. Granqvist, ''Evaporated Sn-doped In_2O_3 Films: Basic Optical Properties and Applications to Energy-Efficient Windows,'' *J. Appl. Phys.*, **60** [11] R123–R160 (1986). □